

## CHAPTER 2

### FRACTURE MECHANICS

#### 1. INTRODUCTION

It has been pointed out in the previous chapter that the HAZ of a weld on 3CR12 consists of at least three different zones, each with a different microstructure and mechanical properties. The properties of the weld metal is determined by the type of filler metal and the dilution with the base metal. Hence, a weldment may therefore be treated as composite specimen which consists of at least five different materials with different properties. Any fracture mechanics analysis of the fracture behaviour of a weldment should therefore be based on the interaction between the different composite materials during loading and fracture. The fusion line or boundary fracture behaviour of welds on 3CR12 represents the most critical part of the fracture behaviour of welds since the fusion line is associated with the HT HAZ which has the lowest toughness.

#### 2. NOTCH-TOUGHNESS TESTING

Masubuchi listed seventeen tests for evaluating the notch-toughness of welds(16). The Charpy V-notch and crack tip opening displacement methods (CTOD) are most commonly used for evaluating the HAZ notch-toughness of welds. Although these two methods are also the most probable methods for determining the notch-toughness of the narrow HT HAZ in 3CR12, they have certain practical limitations. Gooch and Davey have already demonstrated that the toughness of the HT HAZ of welds on 10 mm 3CR12 plate may not be successfully determined with the Charpy V-notch test(13). This is attributed to the following factors:

- a. Even with a K-type weld preparation, Gooch and Davey did not succeed to produce a specimen with a planar HT HAZ which is also oriented normal to the plate surface.
- b. With the size of the HT HAZ very similar to the notch tip radius of the Charpy V-notch, it is very difficult to position the notch tip in the HT HAZ.

In the case of 6 mm 3CR12 and 3CR14 plate, which is the thickness of the plate which was mainly used for this thesis, it is even more difficult to prepare Charpy and CTOD specimens from welded plate which will meet the abovementioned requirements. Another limitation of the Charpy and CTOD methods is the fact that the fusion line fracture initiation behaviour, which is an important aspect of the fracture behaviour of 3CR12 welds, may not be determined with an existing notch or fatigue crack in the HT HAZ.

A new notch-toughness test method was therefore developed (chapter 3) to study the fusion line fracture initiation and propagation behaviour of welds on 6 mm 3CR12 and 3CR14 plate. The notch-toughness of the HT HAZ is characterised by means of a fracture appearance transition temperature (FATT). The transition temperature approach has certain limitations as far as practical implementation of the FATT values are concerned. The FATT, for example, depends on the measurement criteria as well as the thickness of the test specimen. In this study it is used only on a qualitative basis to study the influences of factors like the chemical and phase composition of the HT HAZ, mechanical properties of the different weldment materials, and loading rate, etc., on the fusion line fracture behaviour of welds. The notch-toughness values which were obtained for the HT HAZ of 3CR12 are also compared with values which were determined for both the ferritic stainless steel AISI 409 and mild steel.

### 3. FRACTURE BEHAVIOUR OF WELDS

The resistance of a material to crack extension may be described by means of the stress and strain fields at the crack tip under load. When the material at the crack tip shows linear-elastic behaviour when subjected to a tensile load, the crack tip stress and strain field is described in terms of the stress intensity factor  $K_1$  ( $K_1 = Y\sigma\sqrt{a}$ ). The fracture behaviour of a material may then be predicted by means of linear-elastic fracture mechanics (LEFM). LEFM is, however, only applicable when the crack tip plastic zone is small compared to the crack length and specimen thickness, and usually applies therefore to high strength steels with yield strengths in excess of 1240 MPa(16).

The fracture behaviour of a material, under conditions where crack extension is preceded by extensive plastic deformation, may be predicted

by means of elastic-plastic fracture mechanics (EPFM). The fracture toughness is then described in terms of the crack tip opening displacement (CTOD) parameter, which is actually a measure of the crack tip plastic zone size(17). The J-integral may also be used to characterise the fracture toughness of materials when crack extension is preceded by plastic deformation.

The abovementioned LEFM and EPFM parameters describe the critical crack tip conditions prior to the extension of an existing crack under load in a homogeneous material. Since these fracture toughness parameters were developed to describe the fracture behaviour of a homogeneous material, they may not be used to describe adequately the fracture initiation and propagation behaviour of a composite specimen, e.g. a weldment which consists of different zones with different properties. In the case of a notch on the fusion line of a weld on 3CR12, the stress field ahead of the notch tip during loading will extend into at least three different materials, i.e. the weld metal adjacent to the fusion line, the narrow HT HAZ and fine grained zone in the weld HAZ adjacent to the HT HAZ. It will be demonstrated in this thesis that the fusion line fracture initiation behaviour of defect-free welds and the fracture propagation behaviour of notched welds are critically dependent not only on the fracture toughness, but also on the mechanical properties of the different composite materials of the weldment.

The HAZ fracture behaviour of welds on 3CR12 and 3CR14 plate may therefore be adequately predicted only by means of a fracture theory which will describe the fracture behaviour in terms of the mechanical properties (yield strength, fracture strength, work hardening rate, etc.) of the different composite materials of the weldment. Cottrell and Petch(18) and Davidenkov and Ludwik(19) have respectively developed fracture theories to explain the grain size and temperature sensitive fracture mechanism transitions in steel. In Chapters 3, 4 and 5 it is demonstrated how these theories may also be used to describe the HAZ fracture behaviour of welds on 3CR12 and 3CR14.

### 3.1 Cottrell-Petch fracture theory

Cottrell and Petch used dislocation theory to develop relationships that could account for the effect temperature, grain size and various metallurgical factors have on the likelihood for cleavage fracture for materials that undergo a temperature sensitive fracture mechanism transition. The following relationship was developed for the fracture stress

$$\sigma_f = \frac{4G\gamma_m}{k_y\sqrt{d}} \dots\dots\dots 2.1$$

- where
- $\sigma_f$  = fracture stress
  - $G$  = shear modulus
  - $\gamma_m$  = plastic work around a crack as it moves through the crystal
  - $d$  = grain diameter
  - $k_y$  = dislocation locking term from the Hall-Petch relationship.

Both the fracture stress and yield strength increase with decreasing grain size. Petch demonstrated that the cleavage fracture stress is approximately doubled as the grain size is reduced from a very coarse grain size (250  $\mu\text{m}$ ) to a very fine grain size (25  $\mu\text{m}$ )(20). The Hall-Petch relationship for the yield strength is given by

$$\sigma_{ys} = \sigma_i + \frac{k_y}{\sqrt{d}} \dots\dots\dots 2.2$$

- where
- $\sigma_{ys}$  = yield strength
  - $\sigma_i$  = lattice resistance to dislocation movement resulting from various strengthening mechanisms and intrinsic lattice friction (Peierls stress).
  - $k_y$  = dislocation locking term
  - $d$  = grain diameter

Low demonstrated that the fracture stress is more sensitive to grain size than the yield strength(21). The intersection of the fracture stress and yield stress curves represents a fracture mode transition in

material response. Since the fracture stress and yield stress are temperature sensitive properties, the critical grain size for fracture transition would be expected to vary with temperature. The transition temperature decrease strongly with decreasing grain size.

Tetelman and McEvily studied the significance of the terms in equation 2.1 in more detail and showed that with increasing temperature the fracture stress increases while the yield stress decreases(22). These effects are attributed to an increase in dislocation velocity and a reduction in the Peierls stress. In fact, anything that increases the number of mobile dislocations, their mobility and speed, and the time allowed for such movement, will increase  $\gamma_m$  and the fracture stress.

The temperature dependence of the fracture stress and yield strength is shown in figure 2.1. The intersection of the curves represents a transition in material response. At a temperature  $T_1$  below the transition temperature  $T^*$ , failure must await the onset of plastic flow at the yield strength. With the yield strength at  $T_1$  higher than the fracture stress, an unstable cleavage fracture results in body centered cubic (BCC) materials. At a temperature  $T_2$  above the transition temperature, yielding occurs first and is followed by eventual fracture after a certain amount of plastic flow. Fracture above the transition temperature is usually characterised by a ductile microvoid coalescence mechanism.

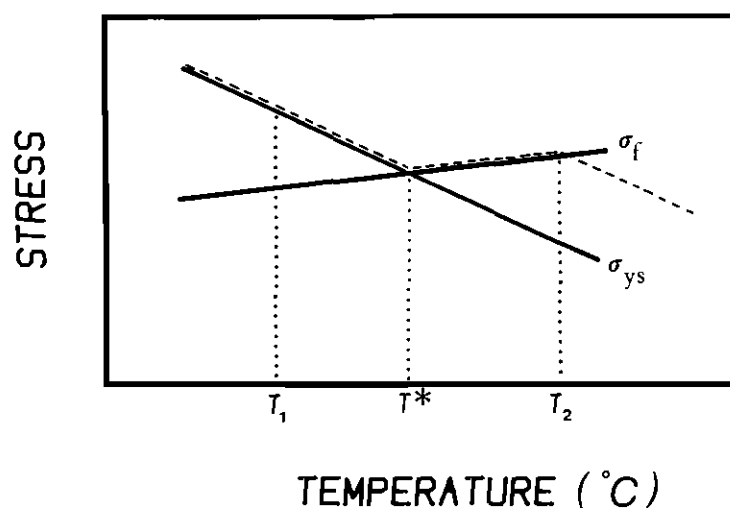


Figure 2.1: Temperature dependence of the fracture stress ( $\sigma_f$ ) and yield strength ( $\sigma_{ys}$ ).

### 3.2 Davidenkov-Ludwik fracture theory

Davidenkov developed a theory for fracture in 1936 which was actually initiated by Ludwik in 1923. They considered plastic flow and fracture to be independent phenomena with yielding obeying a critical shear stress criterion (Tresca), and fracture being dependent on the maximum principal stress. The fracture behaviour of a metal subjected to an uniaxial tensile stress is determined by the relative values of the fracture stress ( $\sigma_f$ ) and flow stress ( $\sigma_{ys}$ ) or yield curves in figure 2.3. The yield stress increases as the material is strain hardened, while the fracture stress is assumed to decrease (fig. 2.3a). Fracture will then occur at the intersection of the curves in figure 2.3a at a strain  $\bar{\epsilon}_1$ .

The relative positions of the flow and fracture stress curves are changed with a change in stress state. The flow stress curve is lowered (according to the maximum shear stress criterion) with the application of a compressive stress  $R$ , perpendicular to the axis of a tensile specimen; while the fracture stress curve is unchanged (maximum principal stress criterion). The intersection of the curves now occur at a greater strain  $\bar{\epsilon}_2$  (fig. 2.3b), corresponding to increased ductility as found in practice with hydrostatic pressure or in a drawing die.

Conversly, a circumferential notch on a tensile test specimen produces tensile stresses perpendicular to the axis, due to the restraint on radial contraction of the material in the notch section by the unyielded material in the full section. The yield curve is therefore raised, giving reduced ductility as shown in figure 2.4

In 1936 Davidenko introduced the cleavage fracture curve ( $\sigma_{CL}$ ) to represent fracture by cleavage (fig. 2.3c); the fracture stress curve ( $\sigma_f$ ) now represents fibrous fracture or fracture by microvoid coalescence. The fracture mode transition from ductile to cleavage fracture with decreasing temperature is now explained, at least qualitatively, since the yield stress of materials which are susceptible to cleavage fracture increases sharply with reduced temperatures. The cleavage fracture curve may now, at lower temperatures, be intersected before the fibrous fracture curve (fig. 2.3c).

This latter situation reflects greater toughness with an increasing ratio of fracture stress to yield strength. This ratio will not increase indefinitely at higher temperatures. A maximum ratio may be correlated with the shelf energy of the Charpy impact energy curve. The shelf energy usually increases with improved steel cleanliness, thus the maximum ratio will also increase with improved steel cleanliness.

If the abovementioned considerations are taken into account a more realistic or correct fracture stress curve may be superimposed on figure 2.1 (dotted curve). Such a fracture stress curve was also obtained by Hahn et al.(19) for unnotched mild steel tensile specimens which were tested within the temperature range  $-250^{\circ}\text{C}$  to  $20^{\circ}\text{C}$  (fig. 2.2).

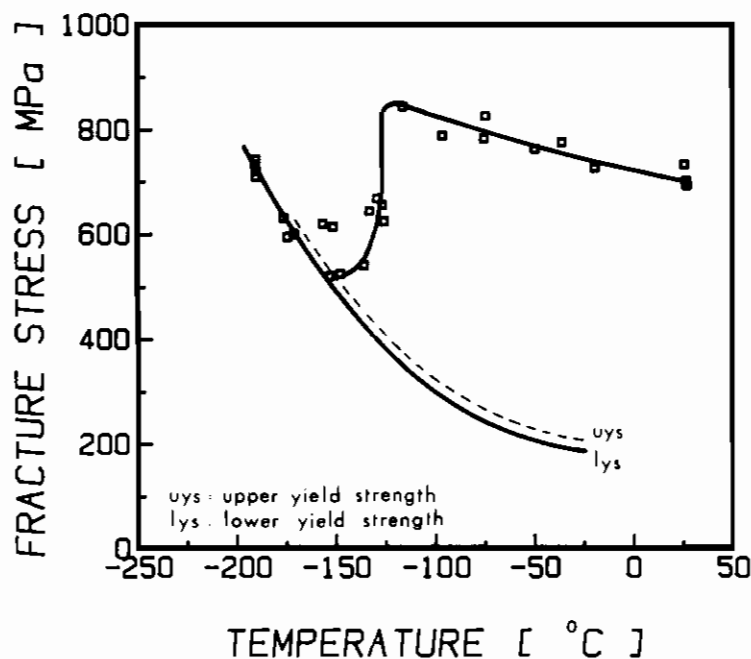


Figure 2.2: Unnotched tensile test data for 0.22 percent carbon steel versus test temperature (After Hahn et al.)

The fracture behaviour of a composite specimen, e.g. a weldment, may now be described by superimposing the fracture and yield stress curves of the different composite materials on the same figure.

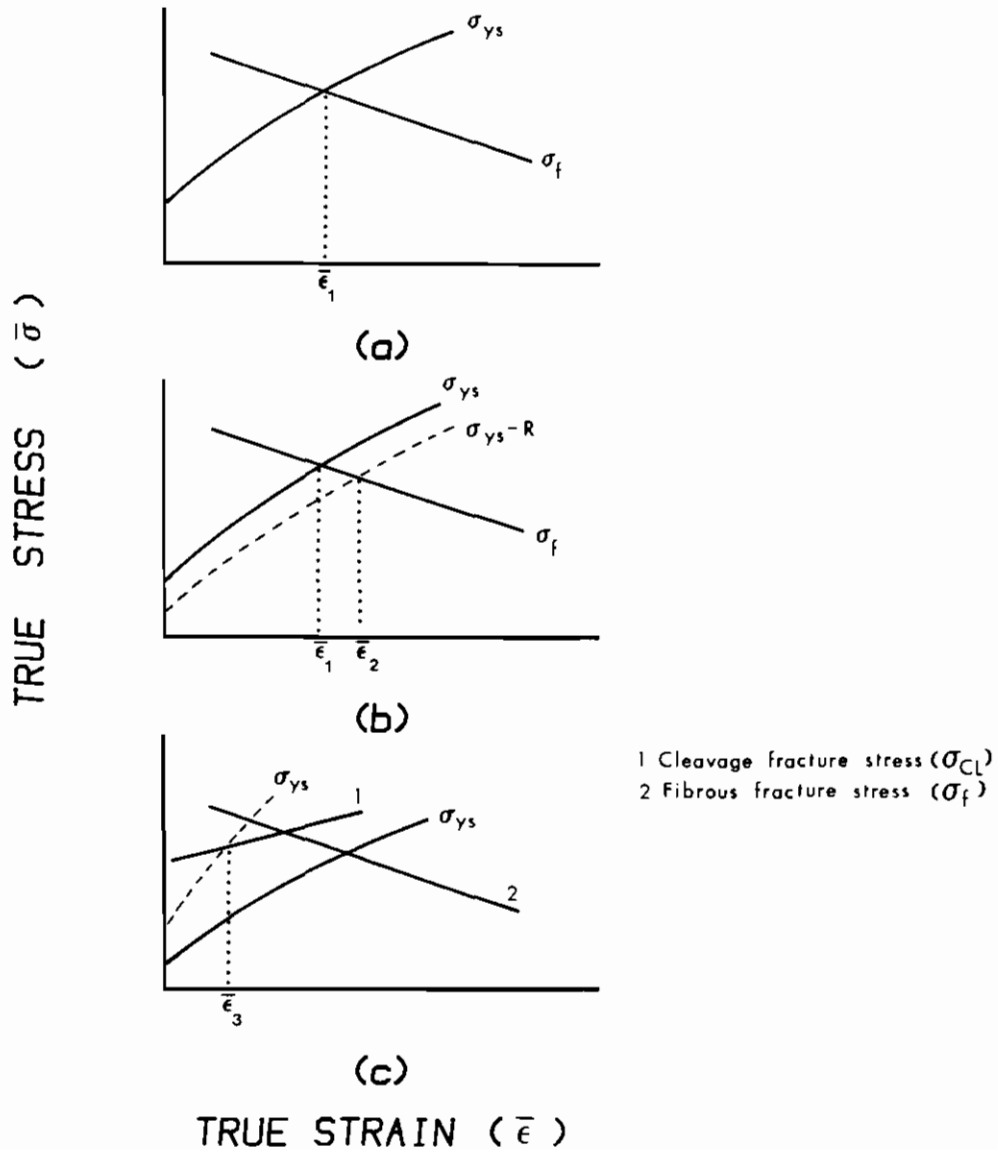


Figure 2.3: a. Fracture ( $\sigma_f$ ) and flow stress ( $\sigma_{ys}$ ) curves for simple tension.  
 b. With a superimposed compressive radial stress  $R$ , the yield curve is shifted to  $\sigma_{ys}-R$  (dotted curve).  
 c. Davidenkov introduced cleavage and ductile fracture curves. The flow stress curve shifts to higher stresses with reducing temperature.



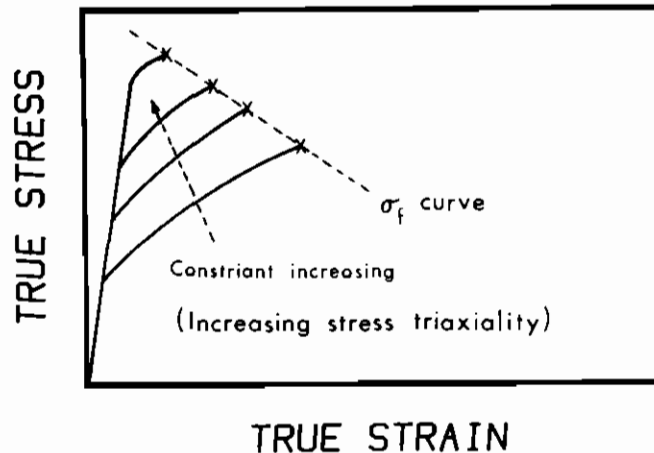


Figure 2.4: Elevation of flow stress ( $\sigma_{ys}$ ) curves with increasing constraint or triaxial stress state.

There is a limit to the extent by which the yield stress or flow stress curve can be raised with increasing constraint. Orowan et al. demonstrated during 1945 to 1948 that the maximum principal stress can only reach three times the tensile yield stress. Thus only those materials for which the cleavage curve is not more than three times the flow stress curve (at test temperature), can be made to undergo cleavage fracture by increasing the degree of restraint. (The factors which determine the cleavage fracture stress have already been discussed.)

The fracture behaviour of a composite specimen may again be described in terms of the mechanical properties of the different composite materials by superimposing the fracture and flow stress curves of the different composite materials on the same figure.